Batteries & Supercaps

Research Article
doi.org/10.1002/batt.202100396

Chemistry Europe
European Chemical Societies Publishing

www.batteries-supercaps.org

Special Collection

Nano-Conductive Additive with Low Interfacial Energy Confining the Movement of Lithium Polysulfide Solution Enables Stable Reaction of Sulfur Electrode in Lithium-Sulfur Batteries

Jong Ho Won,[a] Merry Lee,[b] Hye Min Kwon,[c] and Hyung Mo Jeong*[c]

With the increasing demand for green energy vehicles, lithium-sulfur batteries are drawing attention as new energy storage devices. This is because the theoretical capacity of sulfur cathodes is least five times higher that of conventional cathodes. However, in combination with lithium, sulfur cathodes diffuse to all parts of the cell through an uncontrolled and irreversible shuttle effect. Various studies have attempted to confine sulfur in a particular structure while it is dissolved in electrolytes. Unfortunately, this approach is ineffective because of the mobility and corrosive properties of lithium polysulfide. In this study, we present nano-conductive additives with minimized interfacial energy to lithium polysulfide that controls the shuttle effect by confining the movement of the lithium polysulfide solution within the cathodes. The nano-conductive additive was synthesized to form low interfacial energy through surface modification and used in lithium-sulfur batteries to enable a capacity of approximately 600 mAh g^{-1} for 1000 repeated charge/discharge cycles.

Introduction

The technological requirements for energy storage devices continue to grow owing to their ability to replace generators in difficult and demanding environments.[1] The ideal structure proposed to satisfy the increasing technical requirements is an energy storage device that uses a lithium metal anode, a sulfur cathode, and a solid electrolyte.[2,3] In particular, sulfur cathodes are expected to dramatically improve the performance of energy storage devices because their theoretical capacity is least five times higher that of conventional cathodes.[4,5] However, the sulfur electrode showed insufficient results in the actual application process, and its application to energy storage devices continues to be delayed.[6] As a representative disadvantage, when the sulfur electrode is combined with lithium during discharging, lithium polysulfide is formed, which is easily dissolved in the electrolyte.[5,6] Thus, the amount of the sulfur cathode continues to decrease, as it dissolves and spreads to all parts of the cell through the uncontrollable and irreversible shuttle effect.[5,6] Previous studies attempted to prevent the shuttle effect by enclosing the sulfur cathode in a specific structure;[7–11] however, lithium polysulfide dissolved in the liquid electrolyte easily passed through the confinement structure and spread throughout the cell. In addition, the corrosive nature of lithium polysulfide accelerated the phenomenon by collapsing the structure for confinement.[12] When lithium was removed from lithium polysulfide during subsequent charging of the energy storage device, sulfur, which has poor conductivity, is irregularly precipitated throughout the battery, thus causing serious problems with repeated charge/discharge and stable operation.[13] Therefore, further studies were performed to improve the structural reversibility and conductivity of sulfur cathodes by mixing conductive additives after most part of the electrodes were composed of sulfur, rather than trying to confine sulfur in the structure.[14–18] Although these attempts did not fundamentally improve on the instability of the sulfur electrode, the specific gravity of sulfur constituting the electrode was considerably increased, and continuous conductivity was provided through additives, allowing for the increase in the number of charge/discharge cycles.

Although the fundamental problem with the shuttle effect from the dissolved lithium polysulfide is not avoidable during the repeated charge/discharge of lithium-sulfur batteries (LSBs), confining the movement of lithium polysulfide dissolved electrolytes within cathodes can be considered a practical solution to improve the stability of the overall reaction of LSBs. Since the lithium polysulfide solution is a fluid that can freely move within the cell but is affected by various physical and chemical attractive forces,[19–21] here, we focused on additives

[a] Dr. J. H. Won
Department of Chemistry
Kookmin University
77 Jeongneung-ro, Seongbuk-gu, 02707 Seoul, Republic of Korea
[b] M. Lee
School of Advanced Materials Science and Engineering
Sungkyunkwan University
2066 Seobu-ro, 16419 Suwon, Republic of Korea
[c] H. M. Kwon, Prof. H. M. Jeong
School of Mechanical Engineering and Department of Smart Fab. Technology
Sungkyunkwan University
2066 Seobu-ro, 16419 Suwon, Republic of Korea
E-mail: hmjeong@skku.edu

Supporting information for this article is available on the WWW under https://doi.org/10.1002/batt.202100396

Special Collection *An invited contribution to a Special Collection dedicated to Lithium–Sulfur Batteries.*

Research Article
doi.org/10.1002/batt.202100396
Chemistry Europe
European Chemical Societies Publishing

that could not only play a role in imparting conductivity but could also impact the durability and stability of the electrode structure. In this study, as a method of modifying the surface of the nano-conductive additive (NA), the interfacial energy between the NA and the lithium polysulfide solution is minimized, resulting in the confined movement of the lithium polysulfide solution within the electrode by increased interfacial attraction. The adjusted interfacial energy was measured by observing the wetting angle using the sessile method. The NA with minimized interfacial energy induced the lithium polysulfide solution to remain around the NA. This phenomenon was tested by applying a sulfur cathode with NA to LSBs. In the electrochemical performance of LSBs, NA with minimized interfacial energy to lithium polysulfide solution enabled a longer lifespan and reversibility of LSBs as compared to NA without modification. In addition, through imaging of the electrode after the LSBs reaction, it was confirmed that the sulfur material did not precipitate irregularly and remained homogeneously around the NA despite multiple charging and discharging cycles. This suggests that the additive can be actively used to improve the performance of a sulfur electrode used in an energy storage device, rather than simply providing conductivity to the electrode.

Results and Discussion

Figure 1 shows the wetting angle measurement method for determining the interfacial energy between the lithium polysulfide solution and NA, as well as the information that can be obtained through the measured wetting angle. First, a lithium polysulfide solution was obtained by reacting sulfur and lithium metal in a 1,3-dioxolane (DOL)/1,2-dimethoxyethane (DME) (1 : 1 = v : v) electrolyte in a 3 : 1 weight ratio (Figure 1a). The concentration of the obtained solution was 1 M, based on the weight of sulfur. Since lithium polysulfide is a highly reactive solution, the wetting angle was measured using the sessile drop method in a glove box, as shown in Figure 1(b). Further, Figure 1(c) shows the meaning of the wetting angle measurement results. As shown in Figure 1(c-ii), the wetting angle is determined by the surface tension of the liquid (γ_{LV}), surface energy of the solid (γ_{SV}), and interfacial energy (γ_{LS}) of the two materials, which is described by Young's equation.[22,23]

$$\gamma_{SV} = \gamma_{LS} + \gamma_{LV}\cos\theta \tag{1}$$

The interfacial energy plays an important role in determining the wetting angle. As depicted by the vector in Figure 1(c-ii), when the interfacial energy is close to 0, the contact angle decreases to 0, and the contact angle increases with the increase in interfacial energy.[24] Young's equation can be simply summarized as a wetting coefficient, which can be used to determine whether the surface of a solid can be wetted with a liquid.[25]

$$\omega = \cos\theta = \frac{\gamma_{SV} - \gamma_{LS}}{\gamma_{LV}} \tag{2}$$

In the case of $\omega > 1$, the surface of the solid was completely wetted by the liquid and remained unexposed to air (Figure 1c-

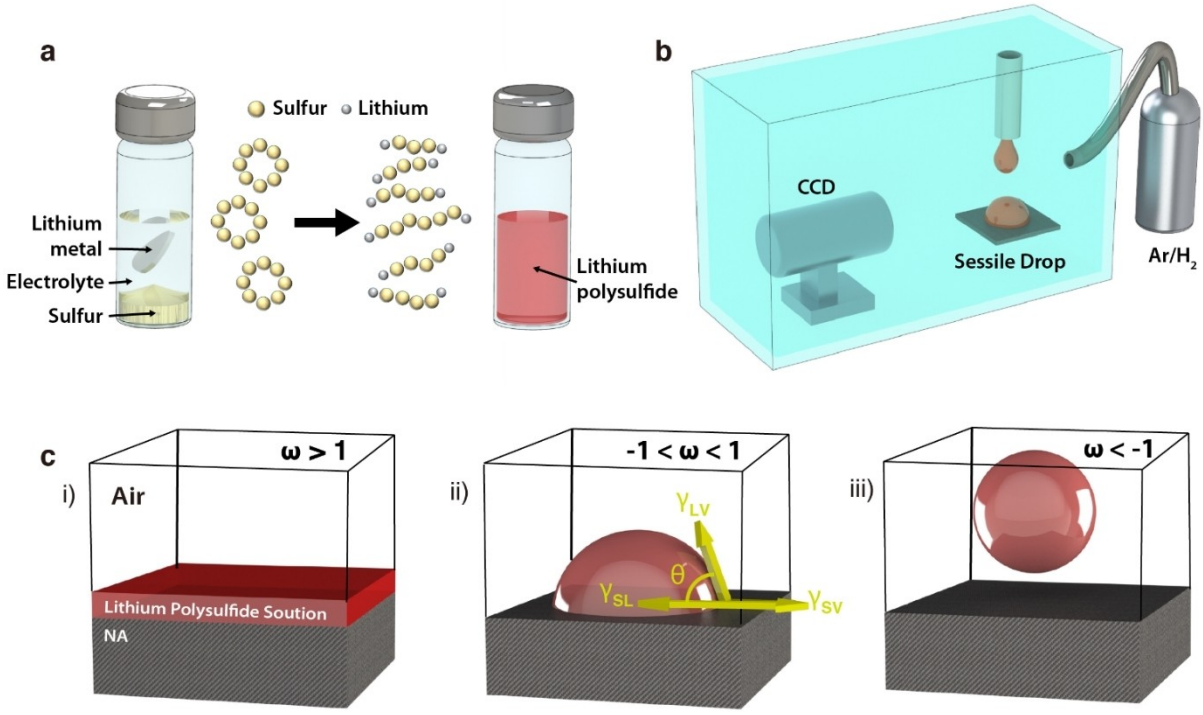

Figure 1. a) Method for synthesizing lithium-polysulfide solution. b) Wetting angle measurement using the Sessile method. c) State of a liquid droplet in equilibrium depending on the wetting coefficient of lithium polysulfide solution and NA: i) $\omega > 1$, ii) $-1 < \omega < 1$, iii) $\omega < -1$.

i). If $\omega < -1$, the surface faces the air, and the liquid is repelled from the solid surface (Figure 1c-iii). If $-1 < \omega < 1$, the liquid will form a certain angle (θ) between the air and the solid surface, as shown in Figure 1(c-ii). As we directly measured the wetting angle, we can immediately determine the affinity of the lithium polysulfide solution with NAs.

In this study, NA was newly synthesized for the sulfur electrode. Conductivity and stability were initially considered the requirements of NA for the sulfur electrode of energy storage device; thus, the usage of carbonaceous NAs was decided. In addition, by making the shape and size of the NA into a sphere of several hundred nanometers or less, the contact with the sulfur electrode was maximized, enabling uniform distribution on the electrode surface. First, resorcinol formaldehyde resin was synthesized by reacting resorcinol and formaldehyde and then was carbonized to produce spherical carbonaceous NA with a size of 300 nm or less, which is called NA0. Upon modifying the surface of NA0, the surface energy is changed, and as a result, a new NA with low interfacial energy concerning lithium polysulfide solution is attempted. According to the definition of surface energy, it is the force through which the successive bonds that consist of a substance try to bond with other substances outside the surface because they cannot find a partner on the surface to bond.[26,27] Therefore, as the surface area of a material increases, the surface energy increases accordingly.[28] We intend to decrease the interfacial energy with lithium polysulfide solution by increasing the surface area of NA0 to increase the surface energy. To increase the surface area of NA0, pore activation using KOH was used.[29] The pore activation process of NA0 is shown in Figure 2(a). First, NA0 and KOH were mixed in a ratio of 1 : 1 by weight and heat-treated for 90 min, while nitrogen flowed through the tube furnace. At this time, the temperature was set at 700 °C, 900 °C, and 1100 °C. The resulting samples were named NA7, NA9, and NA11, as shown in Figure 2(b). The morphologies of NA0, NA7, NA9, and NA11 can be understood through the transmission electron microscope (TEM) data in Figure 2(c) and the scanning electron microscope (SEM) image in Figure S1. According to the photographed microscopic images, NA0, NA7, NA9, and NA11 are spherical carbon structures of 300 nm or less. However, from the TEM data in Figure 2(c) and the SEM cross-sectional image in Figure S1(b), it can be seen that the pore compositions of NA0, NA7, NA9, and NA11 are different. In the case of NA0, pores were hardly visible, and as the heat treatment temperature increased with NA7 and NA9, it was observed that the number of uniform pores in the structure increased. In the case of NA11, it can be confirmed that the carbon structure is partially collapsed owing to the excessively developed pores.[30] After attaching the synthesized NA0, NA7, NA9, and NA11 to the thin film, the wetting angle of the lithium polysulfide solution was measured. It can be seen that the wetting angle decreases from NA0 to NA9, and in the case of NA11, it slightly increases as compared to that of NA9. The exact wetting angles are shown in Figure 2(e). In addition, the specific surface area and pore distribution of NA0, NA7, NA9, and NA11 were measured through nitrogen adsorption experiments. According to the isotherm results in Figure 2(f), the calculated specific surface areas are in the following order: NA9 > NA11 > NA7 > NA0. The specific surface area values are 976 $m^2 g^{-1}$ (NA9), 756 $m^2 g^{-1}$ (NA11), 210 $m^2 g^{-1}$ (NA7), and 66 $m^2 g^{-1}$ (NA0). From the pore distribution in Figure 2(g), it was confirmed that micropores of 10 nm or less developed as the heat treatment temperature increased from NA0 to NA9, and in the case of NA11, macropores increased as the micropores collapsed. Consequently, it can be seen that the increase in pores and specific surface area generated during the heat treatment of NA0 affected the results of the wetting angle measurement, and as the surface area increased, the wetting angle decreased and the interfacial energy with lithium polysulfide significantly decreased. To better understand the interaction between NAs and lithium polysulfide, X-ray photoelectron spectroscopy (XPS) analysis was performed on the NAs (Figure S2). For NA0, C–C bonds of 284.8 eV predominates in investigations for C1s. By contrast, in the process of forming NA7, NA9, and NA11 according to the heat treatment, C–O bonding at 286 eV, C=O at 287 eV, and O–C=O bonding at 288.8 eV continue to increase.[31–33] Increasing the number of oxygen functional groups on the NA surface increases the polar component of the surface energy.[34] Therefore, it plays an important role in lowering the interfacial energy with lithium polysulfide, which is friendly to polar conductors.[35] In the wetting angle test results for the electrolyte without lithium polysulfide, NA7, NA9, and NA11 showed lower wetting angles compared to NA0, indicating that surface modification of NA also increases the affinity with the electrolyte (Figure S3). However, the change is not as dramatic as it is when lithium polysulfide is dissolved, and it can be seen that the surface modification of NAs is particularly effective in increasing the affinity with lithium polysulfide.

The electrochemical performance was evaluated using NA0, NA7, NA9, and NA11 as NA to confirm the effect of each structure on the electrochemical reaction. The NA0, NA7, NA9, and NA11 were mixed with sulfur at a ratio of 1 : 3 by weight (NA : sulfur = 1 : 3). Further, after mixing the material with a binder (10 wt.%), it was attached to a thin metal film and used as a positive electrode and lithium foil as a negative electrode for a 2032 type coin cell. A 1 M LiTFSI in DOL/DME with 0.3 M $LiNO_3$ solution was used as the electrolyte. The graph in Figure 3(a) shows the charge/discharge voltage profiles of the electrodes using NA0, NA7, NA9, and NA11. The electrode using NA9 exhibited an initial discharge capacity of 1,080 mAh g^{-1} at 0.1 C (1 C = 1675 mAh g^{-1}), and 1,001 mAh g^{-1} at 1 C, 825 mAh g^{-1} at 3 C, and 623 mAh g^{-1} at 5 C indicating the best performance among the NAs. Additionally, the electrode using NA9 showed the best rate performance in the rate capability test, as shown in Figure 3(b). The electrode using NA9 operated stably at 5 C, and when it returned to 0.1 C again, it operated normally, and the coulombic efficiency was over 99%. We conducted a long-term charge/discharge test at two rates (1 C, 5 C) using NA9 applied electrodes. In the test conducted at a speed of 1 C, the initial capacity was 987 mAh g^{-1}, and the capacity after 500 cycles was 851 mAh g^{-1}, achieving 86% retention and maintaining a coulombic efficiency of 99% or more. In the long-term test conducted at a speed of 5 C, the

Research Article
doi.org/10.1002/batt.202100396
Chemistry Europe
European Chemical Societies Publishing

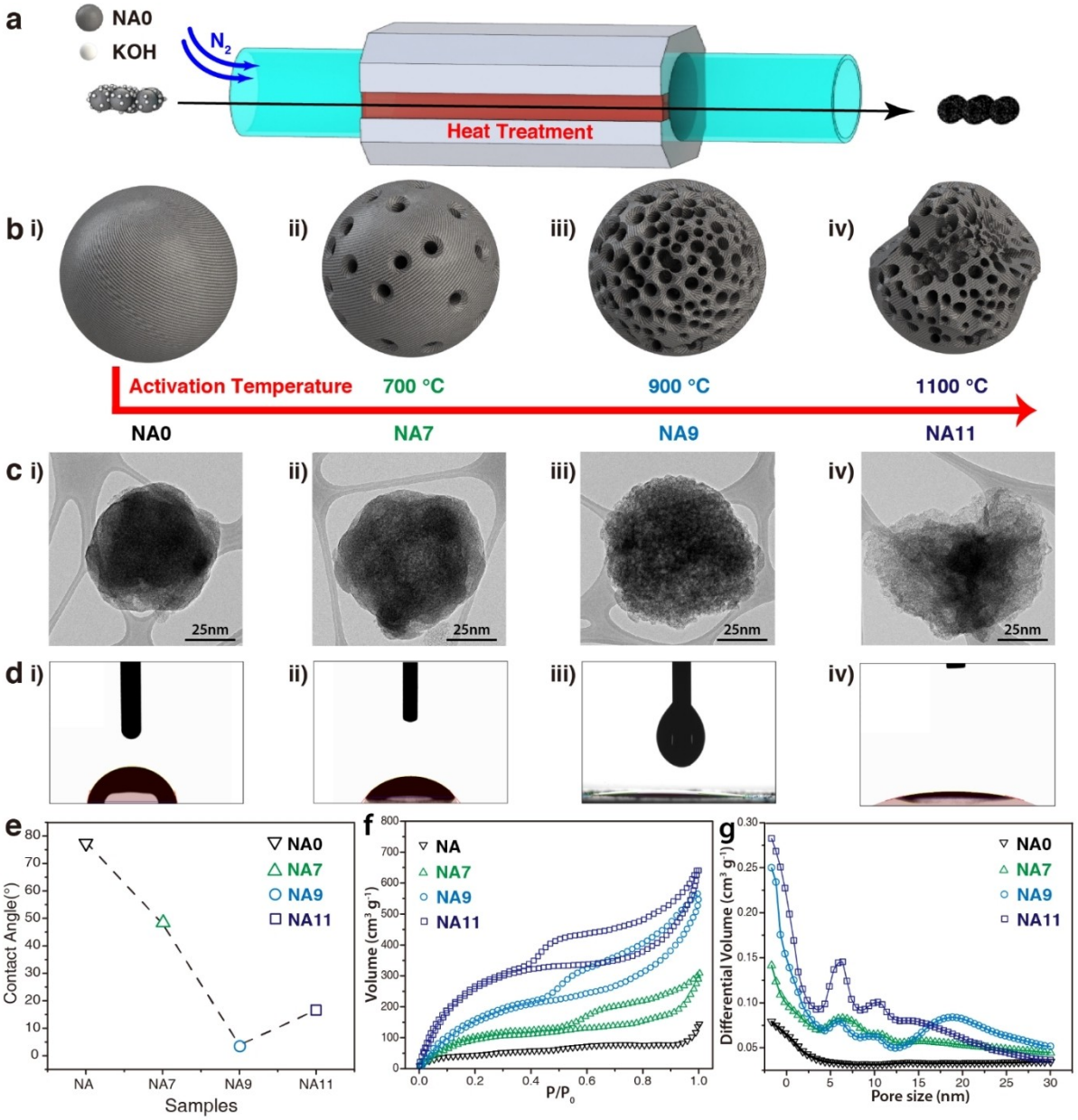

Figure 2. a) Schematic of the NA0 activation method using KOH. b) Schematic and naming of NAs according to the activation temperature. c) Transmission electron microscope (TEM) images of NAs. d) Wetting angle measurements of NAs against lithium-polysulfide solutions. e) Plot of wetting angle measurement results. f) Isothermal graph of nitrogen-adsorption analysis for NAs. g) Pore-distribution plots obtained by nitrogen-adsorption analysis for NAs.

initial capacity was 611 mAh g^{-1}, and the capacity after 1000 cycles was 569 mAh g^{-1}, and 93% retention was achieved. To explain the excellent performance of NA9, the initial surface states of the electrodes using NA0 and NA9 and the surface state after 100 cycles were analyzed by SEM. Both electrodes using NA0 and NA9 are uniformly mixed with sulfur to form a flat surface in the state where the electrochemical reaction is not performed. This is expressed in the schematics of Figure 3(e-i and f-i) and can also be confirmed through the backscattered images of Figure 3(e-ii and f-ii) and the secondary electron images of Figure S4(a-i and b-i). In particular, through the backscattered images of Figure 3(e-ii and f-ii), sulfur particles that are brighter than NAs can be distinguished. During the electrochemical reaction, the sulfur in the electrode repeats the formation of lithium polysulfide and the return to sulfur, as shown in Figure 3(e-iii and f-iii). In this process, an irregular surface area is generally formed as shown in the schematic diagram of Figure 3(e-iv), but NA9 with a large surface area and low interfacial energy with lithium polysulfide solution was expected to induce a flat electrode structure, as shown in Figure 3(f-iv). Backscattered images of Figure 3(e-v and f-v) measured after 100 cycles of electrochemical reaction at a scan rate of 1 C reveal a significant difference. In Figure 3(e-v), it can be seen that the electrode using NA0 has high irregularities due to the irregular precipitation of sulfur. However, in Figure 3(f-v), it is confirmed that the electrode

Research Article
doi.org/10.1002/batt.202100396

Chemistry Europe
European Chemical Societies Publishing

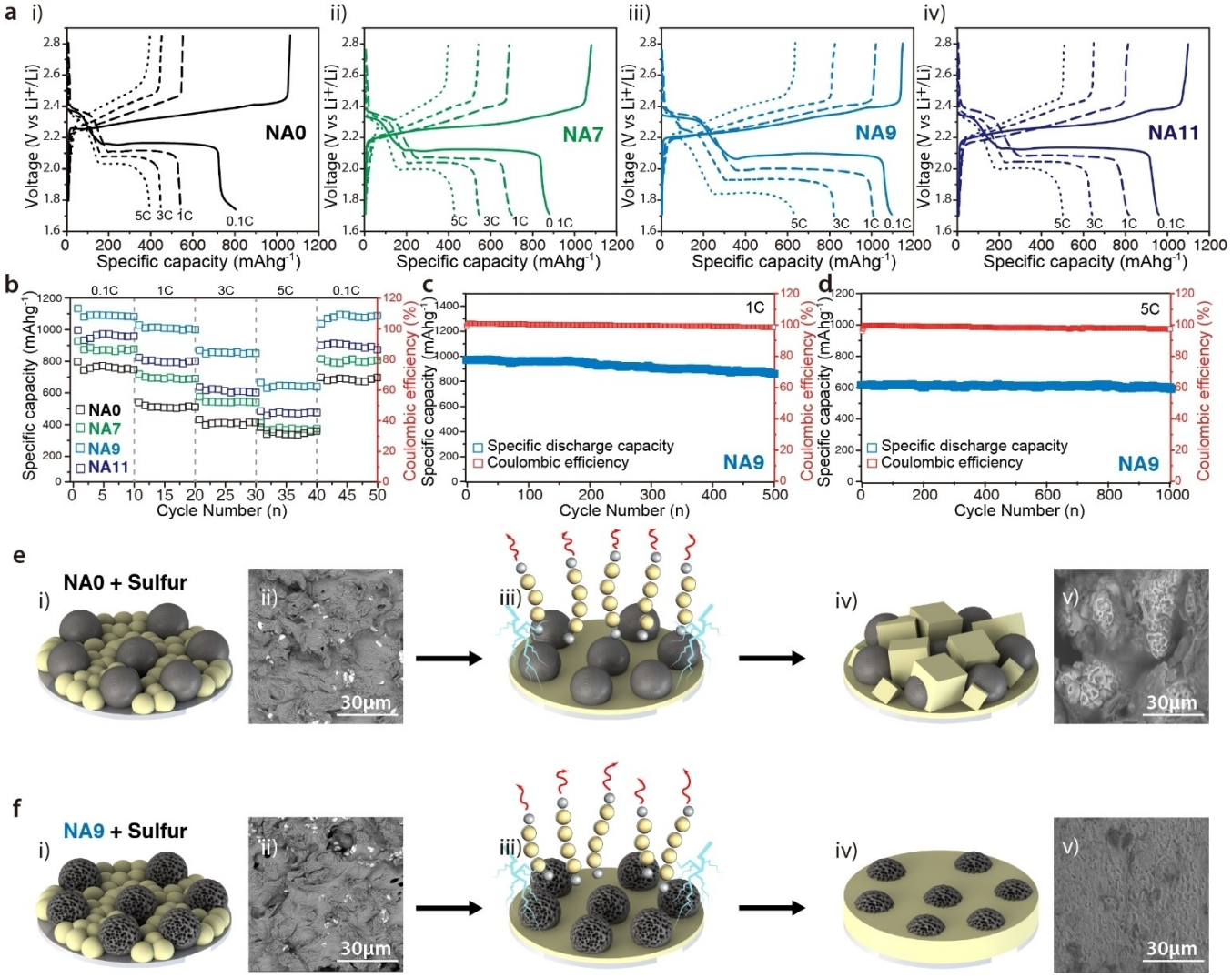

Figure 3. a) Charge/discharge profile of sulfur electrodes with NAs at current densities ranging from 0.1 to 5 C in the potential range of 1.7–2.8 V. b) The rate capability of sulfur electrodes with NAs at current densities ranging from 0.1 to 5 C in the potential range of 1.7–2.8 V. c) Cycling performance of sulfur electrodes with NA9 in the potential range of 1.7–2.8 V at a current rate of 1 C. d) Cycling performance of sulfur electrodes with NA9 in the potential range of 1.7–2.8 V at a high current rate of 5 C, every specific capacity of electrodes was calculated by the total mass of active material and NAs. e) Changes in the electrode surface composed of NA0 and sulfur through an electrochemical reaction: i) Schematic diagram of the initial surface of the electrode. ii) Backscattered scanning electron microscope (SEM) image of the initial surface of the electrode. iii) Schematic during the electrochemical reaction of an electrode. iv) Schematic after electrochemical reaction of electrodes. v) Backscattered SEM image after electrochemical reaction of electrodes. f) Changes in the electrode surface composed of NA9 and sulfur through an electrochemical reaction: i) Schematic of the initial surface of the electrode. ii) Backscattered SEM image of the initial surface of the electrode. iii) Schematic during the electrochemical reaction of an electrode. iv) Schematic after electrochemical reaction of electrodes. v) Backscattered SEM image after electrochemical reaction of electrodes.

using NA9 has a flat structure with a regular attachment of sulfur. These results can also be confirmed through Figure S4(a-ii and b-ii). To confirm that sulfur was uniformly formed due to NA9 even at a high rate of reaction, analysis of electrode morphology was performed at a scanning rate of 5 C. The SEM image in Figure S5 shows the surface of the electrode after 100 cycles of charging and discharging at a scanning rate of 5 C. It can be seen that the sulfur electrode maintains a flat shape, as in the experiment conducted at a scanning rate of 1 C. Figure S6 shows a high-magnification SEM image of the charging process in which sulfur was deposited. Figure S6(a) shows the state of the electrode including NA9 at 2.35 V, in which sulfur is partially deposited. According to the image, it can be seen that the sulfur is deposited thinly and uniformly. As shown in Figure S6(b), uniform deposition is maintained during charging up to 2.8 V. By contrast, Figure S6(c) shows the surface of the electrode including NA0 at 2.35 V. According to the image, sulfur is deposited on the surface in the form of agglomerates, and the agglomerates expand until it reaches 2.8 V (Figure S6d). To evaluate the stability of NA9, we performed the wetting angle test again of lithium-polysulfide solution for NA9 that had undergone a long-term charge and discharge reaction. Figure S7 shows the results of the wetting angle experiment for NA9 after 500 cycles of reaction conducted at scanning rates of 1 C and 5 C, respectively. According to the experimental results, NA9 maintains its affinity

with lithium polysulfide even after a long-term charge/discharge reaction, which proves the stability of NA9. Consequently, NA9 induced a reversible electrochemical reaction of the sulfur electrode in the LSB.

Conclusion

We report a novel additive for the reversible and stable operation of sulfur electrodes for energy storage devices. Surface-modified NAs through pore activation have a high affinity for lithium polysulfide. In particular, NA9 showed low interfacial energy, with lithium polysulfide solution based on a large surface area and high surface energy, and a wetting angle close to zero degrees. Therefore, NA9 was expected to control the irregular movement of lithium polysulfide that occurs continuously in the electrochemical reaction of the sulfur electrode by an attractive force. We evaluated the electrochemical performance of the LSBs using electrodes containing sulfur and NA9. The electrodes containing sulfur and NA9 exhibited specific discharge capacities of 1,080 mAh g^{-1} at 0.1 C and 621 mAh g^{-1} at 5 C, and high Coulombic efficiencies of over 99% were obtained at all charge/discharge rates. In addition, capacity retention was maintained over 500 cycles at 1 C and over 1000 cycles at 5 C. After the electrochemical reaction, a change in the sulfur electrode was observed by analyzing the surface of the electrode. The electrode using NA0, which has a low affinity for lithium polysulfide, had an irregular surface after the reaction. However, the electrode using NA9 had a flat and homogeneous surface even after 100 charge/discharge cycles. NA9 induces uniform precipitation of sulfur and enables a reversible and stable reaction by preventing lithium polysulfide from moving irregularly in the cell and controlling it to remain around the electrode. In conclusion, surface-modified NAs not only imparted conductivity to the sulfur electrode but also increased the structural stability and reversibility during the reaction. Therefore, there is a lot of room for improvement in the performance of energy storage devices through the easy modification of the surface of additives.

Experimental Section

Materials and chemicals

All reagents and chemicals were purchased from commercial sources (US Research Nanomaterials, Aldrich and Duksan) and used without further purification. Sulfur nanoparticles (1–50 nm) were purchased from US Research Nanomaterials, and resorcinol, Pluronic F127, and formaldehyde were purchased from Aldrich. Deionized (DI) water was purchased from Duksan.

Synthesis of the NA0, NA7, NA9 and NA11

NA0 was synthesized by the polymerization of resorcinol and formaldehyde using the sol-gel method. DI water was added to the flask and 120 mmol of formaldehyde and 40 mmol of resorcinol were dissolved. The solution was dissolved while stirring at 90 °C. When dissolution was complete, 4 g of Pluronic F127 and 60 mL of deionized water were added and stirred at room temperature for 12 h. Subsequently, the polymer was separated by centrifugation and dried. The dried polymer was carbonized in a tube furnace and proceeded for 5 h at 600 °C in an inert atmosphere. Further, NA0 and KOH were mixed in a ratio of 1:1 by weight and heat-treated in a tube furnace. Heat treatment was carried out at 700 °C, 900 °C, and 1100 °C for 90 min in an inert atmosphere. After heat treatment, NA7, NA9, and NA11 were obtained.

Material characterization

To investigate the morphology, scanning electron microscope (SEM, SU 8230, Hitachi) and transmission electron microscope (TEM, Talos F200X, FEI) were used. An ion cross-section polisher (IB-09010, JEOL) was used for cross-sectional imaging. Wetting angle measurements (Phoenix-I, Surface Electro Optics) were performed in a glovebox using the sessile method. Nitrogen adsorption–desorption isotherms were obtained using a 3Flex (Micromeritics) instrument. All samples were outgassed at 333 K for 24 h before the measurements.

Electrochemical characterization

A positive electrode was prepared using a slurry that was dispersed in N-methyl-2-pyrrolidone containing elemental sulfur nanoparticles, NA, and a polyvinylidene fluoride binder in a ratio of 68.2:22.7:9.1 by weight. The prepared electrode was dried at 60 °C for 1 h without a forced vacuum. The sulfur loading for each electrode was approximately 2–3.5 mg cm^{-2}. The electrochemical performance of the prepared electrode was evaluated using a CR2032 type coin cell assembled in an argon-filled glove box. For the electrochemical performance evaluation, a lithium metal counter electrode and a Celgard 2400 separator were used. The electrolyte was a mixture of 1,3-dioxolane (DOL) and dimethoxymethane (DME) (v:v = 1:1) with 1 M bis(trifluoromethane)sulfonamide lithium salt (LiTFSI) with 0.3 M $LiNO_3$ solution was used. We used a battery cycler (WonAtech, WBCS-3000) to cycle the electrodes in the potential range of 1.7–2.8 V (vs. Li^+/Li).

Acknowledgements

This work was supported by a National Research Foundation of Korea (NRF) grant funded by the Korea government (MSIT) (NRF-2021R1G1A1011510 and NRF-2021R1A2C4001777). This work was supported by the Nano-Material Technology Development Program through the NRF funded by the MSIT (2009-0082580). This work was also supported by the Technology Innovation Program (20013794, Center for Composite Materials and Concurrent Design) and Korea Institute for Advancement of Technology (KIAT) grant (P0008458, The Competency Development Program for Industry Specialist) funded by the Ministry of Trade, Industry & Energy (MOTIE), Republic of Korea.

Conflict of Interest

The authors declare no conflict of interest.

Research Article
doi.org/10.1002/batt.202100396

Chemistry Europe
European Chemical Societies Publishing

Data Availability Statement

The data that support the findings of this study are available from the corresponding author upon reasonable request.

Keywords: interfacial energy · Li–S battery · nano-conductive additive · surface energy · surface modification

[1] N. Nitta, F. Wu, J. T. Lee, G. Yushin, *Mater. Today* **2015**, *18*, 252–264.
[2] X.-B. Cheng, H.-J. Peng, J.-Q. Huang, R. Zhang, C.-Z. Zhao, Q. Zhang, *ACS Nano* **2015**, *9*, 6373–6382.
[3] B. Ding, J. Wang, Z. Fan, S. Chen, Q. Lin, X. Lu, H. Dou, A. Kumar Nanjundan, G. Yushin, X. Zhang, Y. Yamauchi, *Mater. Today* **2020**, *40*, 114–131.
[4] Y.-X. Yin, S. Xin, Y.-G. Guo, L.-J. Wan, *Angew. Chem. Int. Ed.* **2013**, *52*, 13186–13200; *Angew. Chem.* **2013**, *125*, 13426–13441.
[5] M. Zhao, B.-Q. Li, X.-Q. Zhang, J.-Q. Huang, Q. Zhang, *ACS Cent. Sci.* **2020**, *6*, 1095–1104.
[6] K. Zhu, C. Wang, Z. Chi, F. Ke, Y. Yang, A. Wang, W. Wang, L. Miao, *Front. Energy Res.* **2019**, *7*, 123.
[7] D. Su, M. Cortie, H. Fan, G. Wang, *Adv. Mater.* **2017**, *29*, 1700587.
[8] B. Zhang, C. Luo, G. Zhou, Z.-Z. Pan, J. Ma, H. Nishihara, Y.-B. He, F. Kang, W. Lv, Q.-H. Yang, *Adv. Funct. Mater.* **2021**, *31*, 2100793.
[9] N. Wang, X. Zhang, Z. Ju, X. Yu, Y. Wang, Y. Du, Z. Bai, S. Dou, G. Yu, *Nat. Commun.* **2021**, *12*, 4519.
[10] H. Zhang, L. K. Ono, G. Tong, Y. Liu, Y. Qi, *Nat. Commun.* **2021**, *12*, 4738.
[11] J. H. Won, M. K. Kim, H. M. Jeong, *Appl. Surf. Sci.* **2021**, *547*, 149199.
[12] V. S. Kolosnitsyn, E. V. Karaseva, A. L. Ivanov, *Russ. J. Electrochem.* **2008**, *44*, 564–569.
[13] A. Mistry, P. P. Mukherjee, *J. Phys. Chem. C* **2017**, *121*, 26256–26264.
[14] Q. Pang, X. Liang, C. Y. Kwok, L. F. Nazar, *Nat. Energy* **2016**, *1*, 16132.
[15] H. Ye, J. Sun, S. Zhang, H. Lin, T. Zhang, Q. Yao, J. Y. Lee, *ACS Nano* **2019**, *13*, 14208–14216.
[16] X. Liang, C. Hart, Q. Pang, A. Garsuch, T. Weiss, L. F. Nazar, *Nat. Commun.* **2015**, *6*, 5682.
[17] L. Zhou, D. L. Danilov, R.-A. Eichel, P. H. L. Notten, *Adv. Energy Mater.* **2021**, *11*, 2001304.
[18] H. Ye, J. Y. Lee, *Small Methods* **2020**, *4*, 1900864.
[19] T. Jeon, Y. C. Lee, J.-Y. Hwang, B. C. Choi, S. Lee, S. C. Jung, *Curr. Appl. Phys.* **2021**, *22*, 94–103.
[20] J. H. Yun, J.-H. Kim, D. K. Kim, H.-W. Lee, *Nano Lett.* **2018**, *18*, 475–481.
[21] C. Li, Z. Xi, D. Guo, X. Chen, L. Yin, *Small* **2018**, *14*, 1701986.
[22] T. Young, *Philos. Trans. R. Soc. London* **1805**, *95*, 65–87.
[23] J. H. Won, S. C. Mun, G. H. Kim, H. M. Jeong, J. K. Kang, *Small* **2020**, *16*, 2001756.
[24] L. Makkonen, *J. Phys. Condens. Matter* **2016**, *28*, 135001.
[25] H. Dobbs, D. Bonn, *Langmuir* **2001**, *17*, 4674–4676.
[26] J. Tam, B. Feng, Y. Ikuhara, H. Ohta, U. Erb, *J. Mater. Chem. A* **2018**, *6*, 18384–18388.
[27] P. Müller, A. Saùl, F. Leroy, *Adv. Nat. Sci. Nanosci. Nanotechnol.* **2013**, *5*, 13002.
[28] F. Goujon, A. Dequidt, A. Ghoufi, P. Malfreyt, *J. Chem. Theory Comput.* **2018**, *14*, 2644–2651.
[29] Z. Heidarinejad, M. H. Dehghani, M. Heidari, G. Javedan, I. Ali, M. Sillanpää, *Environ. Chem. Lett.* **2020**, *18*, 393–415.
[30] X. Lan, X. Jiang, Y. Song, X. Jing, X. Xing, *Green Process. Synth.* **2019**, *8*, 837–845.
[31] Y.-C. Chiang, Y.-J. Chen, C.-Y. Wu, *Materials (Basel).* **2017**, *10*, DOI 10.3390/ma10111296.
[32] L. Zhang, L. Tu, Y. Liang, Q. Chen, Z. Li, C. Li, Z. Wang, W. Li, *RSC Adv.* **2018**, *8*, 42280–42291.
[33] D. Ibrahim Abouelamaiem, M. J. Mostazo-López, G. He, D. Patel, T. P. Neville, I. P. Parkin, D. Lozano-Castelló, E. Morallón, D. Cazorla-Amorós, A. B. Jorge, R. Wang, S. Ji, M.-M. Titirici, P. R. Shearing, D. J. L. Brett, *J. Energy Storage* **2018**, *19*, 337–347.
[34] J. Vlček, L. Lapčík, M. Havrdová, K. Poláková, B. Lapčíková, T. Opletal, J. P. Froning, M. Otyepka, *Nanoscale* **2019**, *11*, 3222–3228.
[35] H.-J. Peng, G. Zhang, X. Chen, Z.-W. Zhang, W.-T. Xu, J.-Q. Huang, Q. Zhang, *Angew. Chem. Int. Ed.* **2016**, *55*, 12990–12995; *Angew. Chem.* **2016**, *128*, 13184–13189.

Manuscript received: December 16, 2021
Revised manuscript received: January 21, 2022
Version of record online: February 19, 2022